Nano Research 2018, 11(4): 2229–2236
https://doi.org/10.1007/s12274-017-1842-6
Research Article

ISSN 1998-0124
CN 11-5974/O4

Ion separation and water purification by applying external electric field on porous graphene membrane

Amir Lohrasebi[1,2] (✉) and Samaneh Rikhtehgaran[3]

[1] *Department of Physics, University of Isfahan, Isfahan 81746-73441, Iran*
[2] *School of Nano Science, Institute for Research in Fundamental Sciences (IPM), Tehran 19395-5531, Iran*
[3] *Department of Physics, Florida Atlantic University, 777 Glades Road, Boca Raton, FL 33431-0991, USA*

Received: 17 July 2017
Revised: 14 August 2017
Accepted: 4 September 2017

KEYWORDS

desalination,
nanoporous graphene membrane,
ion separation,
molecular dynamics simulation,
electric field

ABSTRACT

Using molecular dynamics (MD) simulations, a porous graphene membrane was exposed to external electric fields to separate positive and negative ions from salt-water and to produce fresh water. It was observed that, by increasing the strength of the applied electric field, ion separation improved noticeably. In addition, to obtain fresh water, the designed system included two graphene membranes, which are exposed to two external electric fields in opposite directions. Ion rejection was found to be greater than 93% for the electric field of 10 mV/Å and higher. This atomic-level simulation increases the understanding of electric field effects on desalination using multilayer graphene membranes and can be helpful in designing more efficient membranes.

1 Introduction

The lack of sufficient available freshwater resources to meet the growing demand for clean water is currently one of the most worrying global threats. Hence, new techniques and processes should be devised to overcome the problem. Among various desalination technologies for fresh water production, one promising method is membrane desalination via reverse osmosis (RO). Since the desalination performance of RO membranes depends greatly on the structure, operation, and material of the membrane many studies have concentrated on the design of high-performance membranes for water purification. A survey of the relevant literature shows that different membranes—polyamide thin-film composite membranes, metal organic framework (MOF) membranes, such as zeolites [1, 2], covalent triazine framework (CTF) membranes [3, 4], and carbon-based membranes, such as carbon nanotubes (CNTs) [5–8] have been investigated thoroughly. When identifying

---

Address correspondence to lohrasebi@nano.ipm.ac.ir

potential high-efficiency desalination membranes, both water permeability and salt rejection should be considered. Hu et al. showed that polyamide and zeolite membranes can reject salt ions to some extent, while their water permeability is low [1]. It was shown that membranes based on CNTs have high water permeability and high salt rejection [5–8], while Fornasiero et al. proved that the production of highly aligned and high-density CNT arrays is difficult to some extent [9]. Work conducted by Lin et al. on CTF membranes showed that these membranes possess a water permeability of 64.2 L/(cm^2·day·MPa) [4], which is 2–3 orders of magnitude higher than that of current commercially available RO membranes [10]. However, they exhibit poor salt rejection properties.

Functionalized graphene designed computationally by Cohen-Tanugi and Grossman is presented as a novel desalination membrane [11]. They reported that the functionalized nanoporous graphene membranes can provide water transport up to 66 L/(cm^2·day·MPa), with salt rejection exceeding 99%. The water transport of this material is a thousand times faster than conventional reverse osmosis membranes [10], and the graphene membrane still has a high rate of ion rejection. Water permeation through sub-micrometer-thick membranes made from graphene oxide was also studied [12]. In addition, in a more recent experiment, it was shown that single-layer porous graphene can be used as a desalination membrane [13]. Surwade et al. showed that the designed membranes exhibit a salt rejection rate of ~ 100% and rapid water transport. Song et al. prepared a graphene oxide-silver (GO-Ag) nanocomposite with antibacterial activity. They found that GO-Ag nanocomposite is a good candidate for application in water disinfection [14].

Despite their high rate of ion rejection and high water permeability, the use of graphene membranes for water desalination has a few disadvantages. Firstly, ions with a size comparable to that of sodium and chloride ions (e.g. calcium, fluoride and iron) may also be removed in the process of removing salt ions. It should be remembered that these elements are essential to human health. Secondly, the fabrication of graphene membranes is a rather expensive procedure. Thirdly, desalination plants typically have a widespread negative impact on the surrounding eco-system and environment. For instance, most of the brine discharge diffuses back into the marine environment without any further treatment. This can cause considerable environmental destruction, not only in the long term but also in the near future [15, 16].

As an innovative solution to the first disadvantage, water transportation and water purification processes have been investigated under the application of electric fields. The use of electric fields to control nanofluid transport through nanostructures has been reported in literature. It was found that the water flux through the CNT could be controlled significantly by the application of electric fields [17–20]. Meng et al. also demonstrated that the electrostatic field generated by LiF molecules played a significant role in single wall carbon nanotube gating [21]. Li et al. used a rotating electromagnetic field to drive water flow through the nanotube [22]. Furthermore, the ion separation and water desalination under the influence of the electric field produced by a charged CNT surface has been investigated computationally [23].

The effects of electric fields on the water flow rate through carbon nanostructures have been a subject of interest for experimental groups. The importance of the direction of the external electric field in controlling the water flow through the nano-channel has been investigated [24–26]. However, to the author's best knowledge, the use of electric fields to improve the performance of the desalination process based on graphene membranes has not been reported in the literature to date.

In this paper, we suggest a new mechanism based on the application of an external electric field on porous graphene membranes. This method not only increases fresh water production performance but also improves the salt rejection rate. Additionally, it is found that the passage of ions through the porous graphene can be controlled by the application of electric fields, thus providing a possible approach to overcoming the first mentioned disadvantage. For this purpose, the molecular dynamics (MD) simulation method is used to design a highly efficient nano-filter for separating and removing ions from salt-water. The results obtained in this study may shed some light on the unusual fundamental behavior arising at the molecular scale, which could be useful in designing more efficient water purification processes.

2 Experimental

In order to study the influence of external electric fields on ion separation and water purification, computational simulation parts were carried out in two main parts. In the first part, a nano-filter was designed computationally and salt water was pushed toward the filter to separate positive and negative ions under the application of an external electric field. The schematic view of the filter is shown in Fig. 1. In the second part, the results obtained in the first section were used to propose a mechanism for producing fresh water from salt water.

The structure of the system designed in the first part is divided into three (Fig. 1). The first is a reservoir of salt water, box (I), and consisted of a graphene sheet, which acts as a piston and pushes the solution through the graphene membrane. The second division is a membrane consisting of two porous graphene sheets with pore radius of 4 Å and three layers separation distances of *D* = 8, 14, and 20 Å. Box (II) is the third division, and acts as a reservoir for filtered water. The concentration of the solution is 40 g/L of NaCl, which is approximately equal to the salinity of seawater. For this purpose, 30 Na^+ ions, 30 Cl^- ions and about 2,800 water molecules were placed in the simulation box. In this study, all simulations are performed via the LAMMPS package [27] in NVT ensemble at $T = 300$ K by using the Nose–Hoover thermostat. To simulate the dynamics of water molecules, the TIP3P model was used and the interactions between carbon atoms, water molecules, and ions were calculated by employing Lennard–Jones potential. The Lennard–Jones related parameters considered in the Lorentz–Berthelot mixing rule are listed in Table 1 [28]. The long-range electrostatic interactions were computed with the Particle Mesh Ewald method. The equations of motion were integrated via a velocity Verlet method with the time-step of 1 fs, and periodic boundary conditions were imposed in all directions.

As the aim of this study was to explore the effects of an applied external electric field on the performance of the filter, we applied four electric fields of varying intensity along the *z*-direction: E = 100, 10, 1 and 0.1 mV/Å.

In the first part, using the external electric field, the ion separation performance of the filter was discussed. In the second part of our investigations, in order to obtain fresh water, we designed a new structure

Table 1 Lennard–Jones parameters used in the simulations

q (e)	ε (kcal/mol)	σ (nm)	Atom	Type
–0.834	0.1521	0.35364	O	Water
+0.417	0.0460	0.04490	H	Water
0.0	0.0700	0.39848	C	Graphene
+1.000	0.003	0.333	Na	Ions
+2.000	0.006	0.325	Ca	
+2.000	0.014	2.11	Mg	
+1.000	0.003	3.25	K	
–1.000	0.118	0.442	Cl	

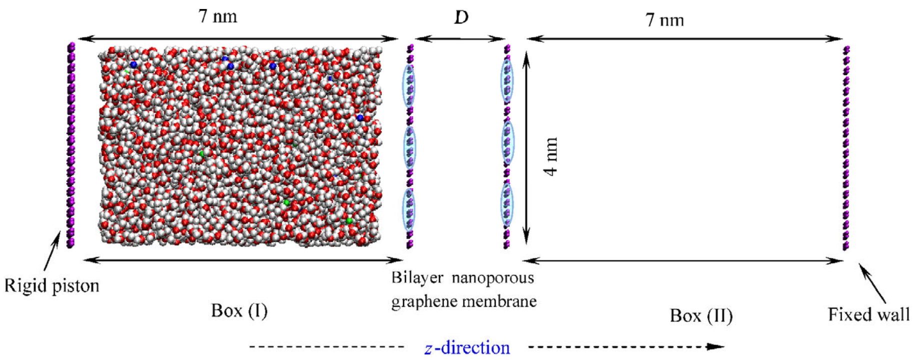

Figure 1 The schematic view of the bilayer porous graphene membrane. The system consists of two reservoirs, boxs (I) and (II), which are separated by a bilayer porous membrane, a movable rigid piston that pushes the salt solution through the membrane and a fixed graphene sheet. The Na^+ and Cl^- ions are shown as green and blue spheres, respectively. The red and white spheres represent oxygen and hydrogen atoms of water molecules, respectively.

consisting of two graphene membranes (the same as the above membrane). These membranes are located between three boxes, as shown in Fig. 2. The first membrane was exposed to a positive *z*-direction electric field, and a similar electric field, with negative *z*-direction, was applied to the second membrane. Since applying the electric fields to the two membranes in opposite directions seems difficult to achieve practically, we propose a new design, shown schematically in Fig. 3, which might be used in a practical approach.

3 Results and discussion

As the first step, we investigated the ion separation efficiency of the graphene membrane. For this purpose, MD simulations were conducted, in which NaCl solution is pushed toward the membrane with the aid of the rigid piston. In the equilibration phase, the piston velocity is kept at zero, and the collection of solution particles is not allowed to pass through the membrane during 1 ns. After the equilibration phase, 5 ns simulations are performed with the piston velocity of $V = 1$ m/s. During the simulation, the piston pushes the solution toward the membrane, causing water molecules to pass through the membrane and enter the second box. As the diameter of the graphene pores is nearly equal to the diameter of hydrated ions, most of the positive/negative ions cannot pass through the membrane. Therefore, they are trapped in the first box and no ion separation occurs in the absence of an external electric field. It was hypothesized that applying an external electric field to the membrane could lead to the separation of the positive and the negative ions. To investigate the influence of an external electric field on the ion separation process and water flow through the membrane, four external electric fields of different intensities (E = 100, 10, 1 and 0.1 mV/Å) were applied along the *z*-direction.

In the presence of an electric field, Na$^+$ and Cl$^-$ ions sustain reverse directional forces along the *z*-direction. Therefore, the probability of passing Cl$^-$ ions through the membrane decreases, while the probability of passing Na$^+$ ions through the membrane increases. To clarify this issue, we briefly describe the overall dynamics of the particles in the simulated system. Most of the hydrated ions in the box (I) cannot pass through the porous membrane, and a few of the ions that are dehydrated can pass through the pores of the graphene membrane. To dehydrate, water molecules must be detached from the ions, which generally requires energy about 6 eV [29]. Since this amount of energy rarely transfers to ions from the surrounding aqueous medium, most of the ions cannot pass through the porous membrane and remain in the box (I). Exposing the system to an external electric field applies a force on the positive ions, which pushes them toward the membrane. Hence, their kinetic energy is increased (for example, about 2 eV at E = 100 mV/Å for D = 2 nm), which leads to an increase in the water-detaching rate from the ions that are close to the membrane pores. Therefore, the entrance probability of Na$^+$ ions to box (II) increases. On the other hand, for Cl$^-$ ions, the applied electric field causes them to move away from the membrane, which decreases the entrance probability of Cl$^-$ ions through the membrane. Therefore, most of the Cl$^-$ions

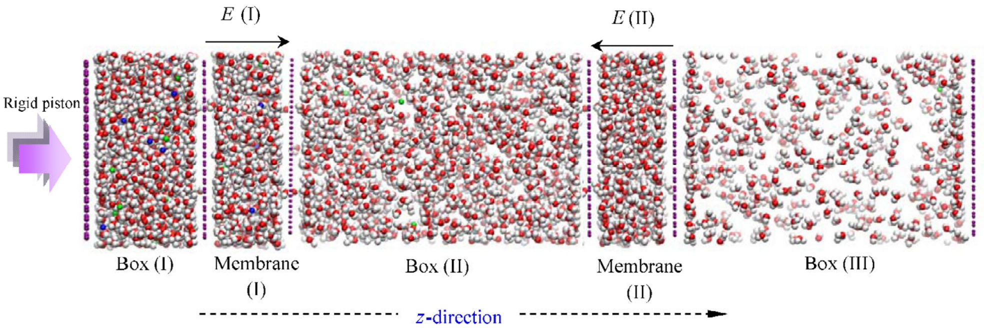

Figure 2 The structure of two-graphene membrane system, which consists of three boxes that are separated by two membranes. A positive electric field, E (I), is applied to the first membrane, and an equal electric field with negative direction, E (II), is applied to the second membrane. The rigid piston pushes the salt solution through the first membrane and then toward the second one.

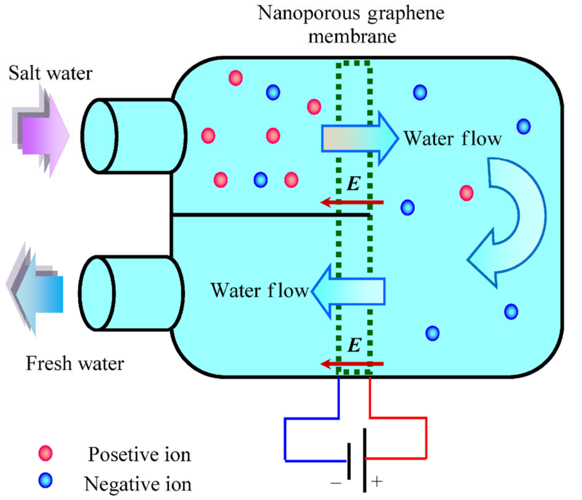

Figure 3 The schematic view of our proposed practical model, which might be useful to design experimental setups of the simulated system. The red and blue spheres represent positive and negative ions, respectively.

remained in box (I), which led to ion separation. To find the minimum value of an external electric field that causes the perfect ion separation, we approximated the free energy of the system, at the beginning and end of the simulations. We know that our system contained $2N$ positive and negative ions. Also, a membrane of thickness D was located between boxes (I) and (II). The free energy variation of the system at fixed temperature is given by Eq. (1)

$$\Delta F = \Delta U - T\Delta S \tag{1}$$

where ΔU and ΔS are the variations of the system's deterministic potential energy and entropy, respectively, due to the application of an external electric field. To obtain the ΔU, we calculate the potential energy variation of the system between the initial configuration in which all the ions are in box (I), and the final configuration in which the positive ions enter box (II), while the negative ions remain in box (I) (i.e. perfect ion separation). In this condition, the potential energy is enhanced by Eq. (2)

$$\Delta U = NeED \tag{2}$$

where e is the electron charge. On the other hand, the change in the entropy of the system between these two configurations is given by Eq. (3)

$$\Delta S = Nk_B \cdot \ln(V_2/V_1) \tag{3}$$

by assuming the ideal gas approximation for the ions (in which k_B is Boltzmann constant, V_2 and V_1 are volume of boxs (I) and (II), respectively). For N = 30, D = 0.8 nm, T = 300 K, and (V_2/V_1) = 3.5, it is easy to show that for an irreversible process ($\Delta F < 0$), the electric field should be greater than 4 mV/Å.

In Table 2 the results of ion separation values for different simulation cases are presented. It can be seen that increasing the strength of applied electric field improves the ion separation for both values of layer separation distances. For an electric field greater than 10 mV/Å, the ion separation is greater than 95%. This is in good agreement with our prediction from the naive estimate free energy variation of the system stated in the previous paragraph.

In addition, the results indicate that the membrane with a larger layer separation distance (D = 20 Å) can separate ions more efficiently. The reason for this may be that the passed ions from the first graphene layer of the membrane with D = 20 Å have more time to be hydrated and to be exposed to the force from the applied electric field. In addition, the percentages of passed water molecules (PPWM) through the membranes with R = 4 Å and D = 8, 14 and 20 Å for different values of E are shown in Table 3. The results show that the PPWM through the membrane with the smaller layer separation distance (D = 8 Å) are higher than those amounts for the membrane with the larger layer distance (D = 20 Å). The smaller volume will be full of the water molecules sooner because the volume

Table 2 Ion separation percentages for NaCl solution with graphene bilayer membrane

R = 4 Å, V = 1 m/s	E = 100 mV/Å	E = 10 mV/Å	E = 1 mV/Å	E = 0.1 mV/Å	E = 0
D = 8 Å	100.0	95.0	56.7	51.7	48.3
D = 14 Å	100.0	96.1	58.2	51.6	49.4
D = 20 Å	100.0	96.7	60.0	51.7	50.0

Table 3 PPWM from graphene bilayer membrane

R = 4 Å, V = 1 m/s	E = 100 mV/Å	E = 10 mV/Å	E = 1 mV/Å	E = 0.1 mV/Å	E = 0
D = 8 Å	71.2	71.0	71.0	71.6	71.7
D = 14 Å	68.9	68.7	67.5	66.2	66.0
D = 20 Å	66.2	66.4	67.1	63.0	63.0

between the graphene layers depends linearly on *D*. Hence, more water molecules flow to box (II) for the system with smaller *D*.

It can be concluded from Tables 2 and 3 that the application of strong electric fields separates ions almost completely and has no significant effect on the water flux through the membrane. In fact, the results show that nanoporous graphene membranes with *D* = 8 Å which are exposed to an electric field of 10 mV/Å can provide water transport of up to 51.8 L/(cm^2·day·MPa), with an ion separation percentage greater than 95%. Since the original seawater solution contains other elements besides Na^+ and Cl^-, such as calcium, potassium and magnesium ions, we studied the performance of the membrane for NaCl, KCl, $CaCl_2$ and $MgCl_2$ solutions. As expected, we obtained results which were similar to those achieved with NaCl solution. The nano filter separates the positive (Na, K, Mg and Ca) and negative ions (Cl^-) from each other with high performance. The results are reported in Table 4. The panels of Fig. 4 show the simulation snapshot for all the system, (a), and for the system without water molecules, (b), after 5 ns simulation time.

We reasoned that by repeating the ion separation process for the passed ions in box (II), fresh water could be obtained (i.e. the particles in box (II) were pushed toward another membrane which is exposed to the same electric field as the first membrane but in the opposite direction). For this purpose, in the second part of our investigation, we designed a system including two membranes, which was mentioned in the Experimental section and is schematically shown in Fig. 2. To consider this process, again, we examine the above four electric field values in our simulations with two membranes. It is observed that by pushing the piston and applying the electric field in the *z*-direction on the first membrane, the solution particles move toward the membrane. During the simulation, it is found that the probability of passing Na^+ ions through the first membrane is more than the probability of passing Cl^- ions. Hence, most of the negative ions remain in the box (I), while most of the positive ions could enter the box (II). Afterwards, particles in box (II) encounter the second membrane exposed to the same strength of electric field but in the opposite direction. In this situation, the passage probability of Na^+ ions across the second membrane is negligible. Therefore, at the beginning, the first box contained NaCl solution. When the piston moved along the *z*-direction, most of the Cl^- ions were trapped in the first box, while most of Na^+ ions remained in box (II), and fresh water was finally obtained in box (III).

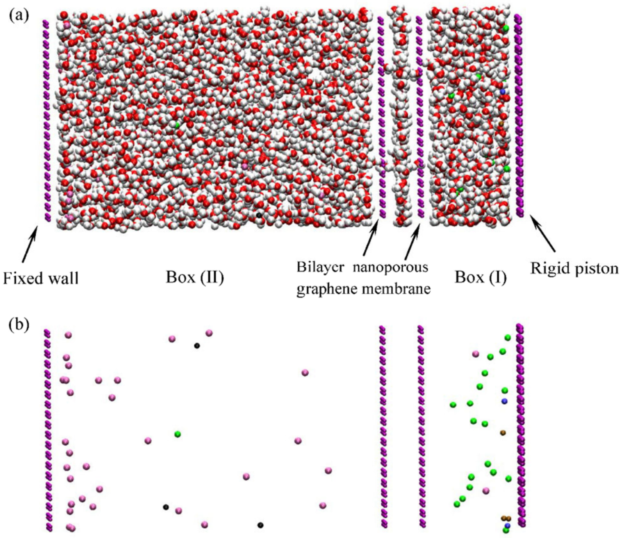

Figure 4 The snapshots of the overall simulation process for NaCl, KCl, $CaCl_2$ and $MgCl_2$ solutions, after 5 ns: (a) all the system and (b) the system without water molecules. Na, Ca, Cl, K and Mg ions are shown by green, brown, pink, blue and black circles, respectively.

Table 4 Ion separation percentages for NaCl, KCl, $CaCl_2$ and $MgCl_2$ solutions and water flow percentages for NaCl solution with different electric direction

R = 4 Å, *V* = 1 m/s	*E* = 100 mV/Å	*E* = 10 mV/Å	*E* = 1 mV/Å	*E* = 0.1 mV/Å	*E* = 0
D = 8 Å	98.3	95.0	52.7	50.8	51.3
PPWM	72.8	73.42	73.0	73.6	73.7

The results of these simulations are shown in Tables 5 to 7. These tables show that by increasing the external electric fields the ion rejection value improves, confirming our expectations. The results indicate that the ion rejection is greater than 93% for an applied electric field of *E* = 10 mV/Å and higher values, which is a great achievement. Figure 3 is a schematic depiction of the case when the ion separation and ion rejection are not 100% (for example for the case that *E* = 10 mV/Å in Table 5). Therefore, some of the positive ions may be seen in the right part of this figure.

Table 5 Ion rejection and water flow percentages for NaCl solution with different electric direction

$R = 4$ Å, $V = 1$ m/s	$E =$ 100 mV/Å	$E =$ 10 mV/Å	$E =$ 1 mV/Å	$E =$ 0.1 mV/Å	$E = 0$
$D = 8$ Å	100	93.5	68.3	67.8	73.3
PPWM	50.7	50.4	50.4	51.2	50.4

Table 6 Ion rejection and water flow percentages for NaCl solution with different electric direction

$R = 4$ Å, $V = 1$ m/s	$E =$ 100 mV/Å	$E =$ 10 mV/Å	$E =$ 1 mV/Å	$E =$ 0.1 mV/Å	$E = 0$
$D = 14$ Å	100	98.7	81.6	71.7	85.0
PPWM	47.8	46.9	46.2	44.8	45.3

Table 7 Ion rejection and water flow percentages for NaCl solution with different electric direction

$R = 4$ Å, $V = 1$ m/s	$E =$ 100 mV/Å	$E =$ 10 mV/Å	$E =$ 1 mV/Å	$E =$ 0.1 mV/Å	$E = 0$
$D = 20$ Å	100	100	85	73.3	86.3
PPWM	45.0	44.1	43.8	39.7	39.7

4 Conclusions

In this study, a system consisting of bilayer porous graphene membrane was designed for ion separation. Our MD simulations show how an external electric field may assist in the ion-separation process. To investigate the effects of applied electric field on the system operation, four electric fields of different intensities were applied to the membrane. The results indicate that by increasing the strength of applied electric field, the ion separation improves significantly. Moreover, according to the obtained results of the first part, we designed a filter composed of two membranes, by applying opposite electric fields in two stages, Na^+ and Cl^- ions are completely removed, and fresh water is produced. It was found that the ion rejection is more than 93% for $E = 10$ mV/Å and higher values of E.

References

[1] Hu, Z. Q.; Chen, Y. F.; Jiang, J. W. Zeolitic imidazolate framework-8 as a reverse osmosis membrane for water desalination: Insight from molecular simulation. *J. Chem. Phys.* **2011**, *134*, 134705.

[2] Gupta, K. M.; Zhang, K.; Jiang, J. W. Water desalination through zeolitic imidazolate framework membranes: Significant role of functional groups. *Langmuir* **2015**, *31*, 13230–13237.

[3] Katekomol, P.; Roeser, J.; Bojdys, M.; Weber, J.; Thomas, A. Covalent triazine frameworks prepared from 1,3,5-tricyanobenzene. *Chem. Mater.* **2013**, *25*, 1542–1548.

[4] Lin, L. C.; Cho, J.; Grossman, J. C. Two-dimensional covalent triazine framework as an ultrathin-film nanoporous membrane for desalination. *Chem. Commun.* **2015**, *51*, 14921–14924.

[5] Zhao, K. W.; Wu, H. Y. Fast water thermo-pumping flow across nanotube membranes for desalination. *Nano Lett.* **2015**, *15*, 3664–3668.

[6] Das, R.; Ali, M. E.; Hamid, S. B. A.; Ramakrishna, S.; Chowdhury, Z. Z. Carbon nanotube membranes for water purification: A bright future in water desalination. *Desalination* **2014**, *336*, 97–109.

[7] Majumder, M.; Chopra, N.; Andrews, R.; Hinds, B. J. Nanoscale hydrodynamics: Enhanced flow in carbon nanotubes. *Nature* **2005**, *438*, 44.

[8] Kar, S.; Bindal, R. C.; Tewari, P. K. Carbon nanotube membranes for desalination and water purification: Challenges and opportunities. *Nanotoday* **2012**, *7*, 385–389.

[9] Fornasiero, F.; In, J. B.; Kim, S.; Park, H. G.; Wang, Y. M.; Grigoropoulos, C. P.; Noy, A.; Bakajin, O. pH-tunable ion selectivity in carbon nanotube pores. *Langmuir* **2010**, *26*, 14848–14853.

[10] Oyama, S. T.; Stagg-Williams, S. M. *Inorganic, Polymeric and Composite Membranes*; Elsevier: Amsterdam, The Netherlands, 2011.

[11] Cohen-Tanugi, D.; Grossman, J. C. Water desalination across nanoporous graphene. *Nano Lett.* **2012**, *12*, 3602–3608.

[12] Nair, R. R.; Wu, H. A.; Jayaram, P. N.; Grigorieva, I. V.; Geim, A. K. Unimpeded permeation of water through helium-leak-tight graphene-based membranes. *Science* **2012**, *335*, 442–444.

[13] Surwade, S. P.; Smirnov, S. N.; Vlassiouk, I. V.; Unocic, R. R.; Veith, G. M.; Dai, S.; Mahurin, S. M. Water desalination using nanoporous single-layer graphene. *Nat. Nanotechnol.* **2015**, *10*, 459–464.

[14] Song, B.; Zhang, C.; Zeng, G. M.; Gong, J. L.; Chang, Y. N.; Jiang, Y. Antibacterial properties and mechanism of graphene oxide-silver nanocomposites as bactericidal agents for water disinfection. *Archiv. Biochem. Biophys.* **2016**, *604*, 167–176.

[15] Lattemann, S.; Hoepner, T. Environmental impact and impact assessment of seawater desalination. *Desalination* **2008**, *220*, 1–15.

[16] Song, B.; Zeng, G. M.; Gong, J. L.; Liang, J.; Xu, P.; Liu, Z. F.; Zhang, Y.; Zhang, C.; Cheng, M.; Liu, Y. et al. Evaluation

methods for assessing effectiveness of *in situ* remediation of soil and sediment contaminated with organic pollutants and heavy metals. *Environ. Int.* **2017**, *105*, 43–55.

[17] Ritos, K.; Borg, M. K.; Mottram, N. J.; Reese, J. M. Electric fields can control the transport of water in carbon nanotubes. *Phil. Trans. R. Soc. A: Math. Phys. Eng. Sci.* **2016**, *374*, 20150025.

[18] Su, J. Y.; Guo, H. X. Control of unidirectional transport of single-file water molecules through carbon nanotubes in an electric field. *ACS Nano* **2011**, *5*, 351–359.

[19] Ghadamgahi, M.; Ajloo, D. Molecular dynamics simulation of the water transportation through a carbon nanotube. The effect of electric field. *Russ. J. Phys. Chem. A* **2015**, *89*, 2120–2125.

[20] Rinne, K. F.; Gekle, S.; Bonthuis, D. J.; Netz, R. R. Nanoscale pumping of water by AC electric fields. *Nano Lett.* **2012**, *12*, 1780–1783.

[21] Meng, X. W.; Wang, Y.; Zhao, Y. J.; Huang, J. P. Gating of a water nanochannel driven by dipolar molecules. *J Phys. Chem. B* **2011**, *115*, 4768–4773.

[22] Li, X. P.; Kong, G. P.; Zhang, X.; He, G. W. Pumping of water through carbon nanotubes by rotating electric field and rotating magnetic field. *Appl. Phys. Lett.* **2013**, *103*, 143117.

[23] Rikhtehgaran, S.; Lohrasebi, A. Water desalination by a designed nanofilter of graphene-charged carbon nanotube: A molecular dynamics study. *Desalination* **2015**, *365*, 176–181.

[24] Figueras, L.; Faraudo, J. Competition between hydrogen bonding and electric field in single-file transport of water in carbon nanotubes. *Mol. Simul.* **2012**, *38*, 23–25.

[25] Zhu, J. Z.; Lan, Y. Q.; Du, H. J.; Zhang, Y. H.; Su, J. G. Tuning water transport through nanochannels by changing the direction of an external electric field. *Phys. Chem. Chem. Phys.* **2016**, *18*, 17991–17996.

[26] Winarto; Takaiwa, D.; Yamamoto, E.; Yasuoka, K. Structures of water molecules in carbon nanotubes under electric fields. *J. Chem. Phys.* **2015**, *142*, 124701.

[27] Plimpton, S. Fast parallel algorithms for short-range molecular dynamics. *J. Comput. Phys.* **1995**, *117*, 1–19.

[28] Allen, M. P.; Tildesley, D. J. *Computer Simulation of Liquids*; Oxford University Press: New York, 1987.

[29] Armstrong, C. M. Reflections on selectivity. In *Membrane Transport*; Tosteson, D. C. Ed.; Springer: Berlin, Germany, 1989; pp 261–273.